

Magnetic-flux periodic response of nanoporated ultrathin superconducting films

M. D. Stewart, Jr., Zhenyi Long, and James M. Valles, Jr.
 Department of Physics, Brown University, Providence, Rhode Island 02906, USA

Aijun Yin and J. M. Xu
 Division of Engineering, Brown University, Providence, Rhode Island 02906, USA

(Received 13 October 2005; revised manuscript received 12 January 2006; published 20 March 2006)

We have patterned ultrathin Bi/Sb films with a hexagonal array of nanoscale holes. These regular perforations result in a phase-sensitive periodic response to an applied magnetic field. Thus by measuring this response in the resistive transitions we are able to distinguish between superconducting fluctuations of the amplitude and phase. Our results delineate three distinct portions of the $R(T)$ in which fluctuations of the amplitude, both the amplitude and phase, and the phase of the superconducting order parameter dominate. In addition, as T_{c0} is lowered the region of the superconducting transition dominated by amplitude fluctuations is large and grows with proximity to the superconductor to insulator transition.

DOI: 10.1103/PhysRevB.73.092509

PACS number(s): 74.40.+k, 74.25.Qt, 74.78.-w, 74.81.Fa

The superconductors originally considered by BCS exhibited spectacularly sharp transitions from a finite resistance to zero resistance as a function of temperature.¹ Fluctuation effects were negligible. Presently, a great deal of attention focuses on low superfluid density superconductors for which fluctuations strongly influence and substantially broaden their phase transitions. These include the high temperature superconductors,² and in particular, their underdoped versions,³⁻⁵ and ultrathin superconducting films near the superconductor to insulator transition (SIT).⁶⁻¹⁰ For the latter, resistive transitions, $R(T)$, can develop widths comparable to or greater than the apparent mean field transition temperature, T_{c0} .¹¹

To discuss the effects of fluctuations on the $R(T)$ it is helpful to consider the two component superconductor order parameter $\psi = |\psi_0|e^{i\phi}$. In bulk elemental superconductors, the sharp $R(T)$ reflect the near simultaneous appearance of a finite amplitude, $|\psi_0|$, and long range coherence of the phase, ϕ . In low superfluid density superconductors, however, the amplitude first forms at high temperatures and phase coherence develops at lower temperatures.^{2,12-14} High on a transition quasiparticles transiently form Cooper pairs, which enhances the quasiparticle or fermionic contribution to the conductivity, σ_f . These pair or amplitude fluctuations give rise to the initial drop in $R(T)$.¹⁵ At very low values of R , a substantial Cooper pair density exists and the conductivity of these bosons, σ_b , controls $R(T)$. σ_b is limited by the motion of vortices which causes fluctuations in the phase of the Cooper pair condensate. In between, a two fluid model may best describe the transport.⁷

Physical interpretations of the $R(T)$ in high sheet resistance films especially those near the SIT rely heavily on distinguishing the amplitude and phase fluctuation dominated regimes.³⁻⁶ Most often, explicit models for $\sigma_f(T)$ and $\sigma_b(T)$ do not exist as a guide and qualitative arguments must prevail. In this paper we present the magnetic flux response of the $R(T)$ of a series of very low superfluid density (high sheet resistance)^{11,16} films patterned with a nanoscale array of holes. We use the quality of the flux response at different points along their transitions to determine the presence of

well-defined vortices¹⁷ and thus provide insight into where the amplitude fluctuation dominated transport gives over to phase fluctuation dominated transport. In addition, we propose that this method can be used to directly detect the existence of vortices in settings where their presence has been contentious.⁸

As a consequence of phase coherence, magnetic field periodic behavior is expected in films with multiply connected periodic geometries (see inset of Fig. 1).^{18,19} For example, the resistive transitions of thick Nb films²⁰ on nanopore arrays and thick Al films with much larger lattice and hole dimensions²¹ oscillate in temperature while maintaining their shape in an applied magnetic field. For holes separated by segments of width ξ_0 or more²⁰

$$\frac{\Delta T_c}{T_{c0}} = - \left(\frac{\xi_0}{a} \right)^2 \left[\frac{1}{4} - \left(\frac{\phi}{\phi_0} - n - \frac{1}{2} \right)^2 \right], \quad (1)$$

where ΔT_c is the shift in the transition, ξ_0 is the (dirty) coherence length, a is the hole to hole spacing,²² n is an integer, and ϕ is the applied magnetic flux. $\phi_0 = H_m \left(\frac{\sqrt{3}}{2} a^2 \right)$ is the magnetic flux corresponding to having one flux quantum per unit cell and defines the unit cell matching field, H_m .

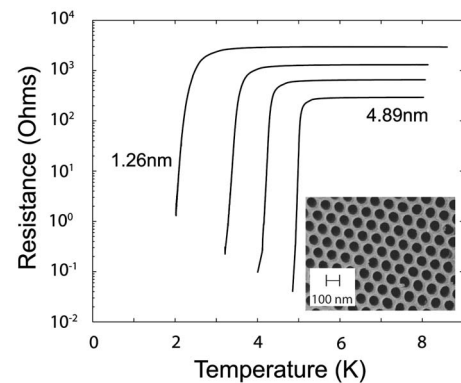


FIG. 1. Superconducting transitions for a perforated film. Inset shows an SEM image of one of the substrates used in these experiments. The hole lattice constant is $a = 100$ nm and $R_{\text{hole}} = 33$ nm.

Equation (1) is derived within the context of mean field theory, or in the absence of appreciable fluctuations of the superconducting order parameter and without considering vortex motion. Therefore the physical picture which leads to Eq. (1) is that of immobile vortices which penetrate the film through the array of holes. These vortices generate screening currents which, at $H=nH_M$, nearly cancel in the interior of the film so that $\Delta T_c \approx 0$. At incommensurate fields the screening currents give rise to pair breaking and thus a reduction in T_c . The microscopic picture described by Eq. (1) is the familiar Little-Parks physics.

Equation (1) accounts well for the flux periodic behavior of thick Nb films.²⁰ However, it has been shown in wire arrays that fluctuations invalidate this picture, introducing an oscillation amplitude that depends on $r=R/R_N$.²³⁻²⁵ Amplitude fluctuations prevent the formation of screening currents as described above when the fraction of the normal state resistance is greater than some particular value. Typically, this value is $r_0 \geq 0.5$.²³⁻²⁵ Our data on ultrathin low superfluid density films show this situation can persist as low as $r_0=0.24$ in the lowest T_{c0} film. In addition, our data show that as r decreases ($r \leq 0.15$) and screening currents appear, the films' susceptibility to thermal fluctuations allows activated vortex motion to dominate the transition. The data, therefore, indicate that the region of the transition dominated by amplitude fluctuations grows with decreasing T_{c0} and hence increasing proximity to the SIT.

Our experiments were conducted on homogeneous quench condensed Bi/Sb films similar to those employed in previous studies of the SIT and thermally activated flux flow (TAFF).¹¹ These films have very low superfluid density because they are thin and disordered.^{11,16} Two films were made simultaneously for each experiment. One film was deposited on a fire-polished glass substrate while the other was deposited on a nanoporated anodic aluminum oxide (AAO) substrate (see the inset of Fig. 1). The latter assumed the honeycomb geometry of the substrate. This *in situ* fabrication method allows us to vary film parameters such as T_{c0} while completely circumventing problems encountered when comparing films on different substrates. The preparation of the AAO substrates can be found elsewhere in the literature.²⁶⁻²⁹ Those used in these experiments had a hole lattice constant, a , of 100 nm and a hole radius, $R_{\text{hole}}=33$ nm. Both substrates were precoated with 50 nm of thermally evaporated Ge (in an attempt to smooth the small surface roughness of the AAO substrate) before Au contact pads were deposited at room temperature. Subsequently both substrates were mounted in our cryostat where a series of homogeneous Bi films were fabricated at $T=8$ K by first evaporating a thin film of Sb (<1 nm, which ensures the films' homogeneous morphology) and then depositing the desired thicknesses of Bi through sequential depositions. In this way, a series of Bi films were fabricated without breaking vacuum or warming.

The $R(T)$ were measured using standard four-terminal, low-frequency ac techniques and acquired in the regime of applied currents where the films exhibit an ohmic response. Nonlinearities associated with the phase transition to the zero resistance state, which are expected at lower temperatures and have been observed in some wire arrays, do not appear in this experiment's range.^{23-25,30-32} The normal state resis-

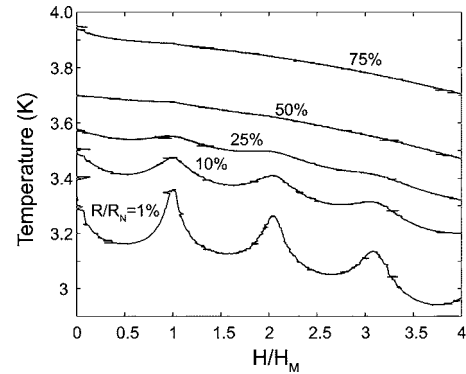


FIG. 2. Isodissipative measurements of temperature vs magnetic field (normalized by the matching field) for a representative perforated film with $d_{\text{Bi}}=1.90$ nm, $T_{c0}=3.70$ K, $r_{\text{hole}}=33$ nm, and hole spacing $a=100$ nm. Inset shows the corresponding superconducting transition with the arrows indicating the value of R/R_N where the curves in the main panel were taken. Equation (1) predicts that each curve should exhibit the same magnitude oscillation of ≈ 0.01 K.

tances, R_N , of neighboring film regions were compared to assess film homogeneity and found to agree to $<7\%$. Magnetic fields were applied perpendicular to the planes of the films. Our thermometry consists of a calibrated carbon glass resistor which has a negligible magnetoresistance in the range of fields used in these experiments.

Data from a series of four superconducting films with T_{c0} ranging from 2.65 to 5 K and normal state resistances, $R_N=R(8$ K), ranging from 3.3 k Ω to 300 Ω are shown in Fig. 1. The reference film exhibits the same range of T_{c0} and a similar increase in the widths of its transitions with decreasing T_{c0} . The latter characteristic has been ascribed to a growing fluctuation dominated regime.¹¹ The systematic reduction in T_{c0} is believed to result from disorder enhanced Coulomb repulsion effects that grow with increasing R_N and possibly drive the SIT.^{33,34}

Despite the breadth of the superconducting transitions they do oscillate with increasing magnetic field. The amplitude of the oscillations, however, depends strongly on the reduced resistances, $R(T)/R_N$, at which they are measured. That is, unlike thicker films the shape of the transitions change in field.^{20,21,23} Figure 2 shows a typical series of isodissipative (i.e., fixed r) measurements of ΔT .³⁵ (R_N does not change in this range of applied fields.) The lower r curves exhibit oscillations that diminish in size with increasing field and are superimposed on a nearly quadratic background. The peaks in the data appear at $H=nH_M=n(2145 \pm 50)$ Gauss where n is an integer. H_M corresponds closely to the calculated value for one flux quantum per unit cell of the hole array (see Ref. 22). Thus these oscillations result from the collective response of the hole array rather than from the responses of single holes.³⁶ A feature of particular interest is that the peak amplitudes are larger at lower r .

We characterize the flux periodic response using a normalized oscillation amplitude, A , for the first oscillation:

$$A = \frac{T(r,0) + T(r,H_M)}{2T_{c0}} - \frac{T(r,H_M/2)}{T_{c0}}. \quad (2)$$

Each solid curve of A as a function of r shown in Fig. 3 was calculated using individual measurements of $R(T)$ at 0,

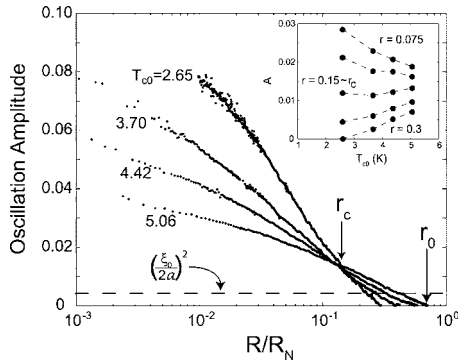


FIG. 3. Normalized amplitude of the first temperature oscillation as a function of fractional resistance for four perforated films with $2.65 < T_{c0} < 5.06$ K, $R_{\text{hole}}=33$ nm, and $a=100$ nm. Inset shows the unexpected behavior of the $A(r)$ with T_{c0} near r_c .

$H_m/2$, and H_m . The dashed curve represents the mean field oscillation amplitude, $A_{MF}=(\xi_0/2a)^2$, derived from Eq. (1). $\xi_0 \approx 10$ nm represents the average value for these films as determined from measurements of the upper critical fields of the reference films. It varied by 20% over this range of T_{c0} .

The oscillation amplitudes exhibit a rich dependence on r and T_{c0} , unlike the constant mean field prediction. For all T_{c0} , A grows nearly logarithmically from zero with decreasing r with a dependence that is stronger for the films with lower T_{c0} . For $r \ll 1$, the oscillations surpass 10 times the mean field result. The r at which oscillations first appear, r_0 , is well defined and is lower for lower T_{c0} . Interestingly, the $A(r)$ for different T_{c0} cross in the vicinity of a single point near $r=r_c \approx 0.15$. The existence of this crossing point is supported by data on another hole size. Its significance is brought out partially by the inset in Fig. 3, which shows how A depends on T_{c0} at fixed values of r . r_c delineates the portions of the $R(T)$ in which A increases or decreases with the primary energy scale characterizing the transition, T_{c0} .

Accounting for the very large A at low r and the vanishing of A for $r \approx \frac{1}{2}$ clearly requires consideration of the effects of fluctuations.^{23,37} Unfortunately, detailed theoretical predictions for the $R(T)$ do not exist. Our identification of two scales in the data, r_0 and r_c , however, provide a useful guide for the discussion. As we emphasize below, the two scales define points on the transitions at which the dissipative processes and character of the fluctuation effects qualitatively change.

Insight into the large amplitude of the oscillations at $r < r_c$ comes from investigating the tails of the superconducting transitions in magnetic field. Figure 4 shows Arrhenius plots of the $R(T)$ collected at $H=0$, $H_M/2$, and H_M for two films with different T_{c0} . The tails of the $R(T)$ follow

$$R(T) = R_0 e^{(-T_0/T)}, \quad (3)$$

which is the signature of thermally activated flux flow (TAFF). The energy barrier, T_0 , is lower by more than a factor of 2 at $H=H_M/2$ than at $H=H_M$. This nonmonotonic variation in T_0 gives rise to the ΔT oscillations that continuously grow as $r \rightarrow 0$. At $H=H_M$ the vortices come into registry with the holes and thus their lattice is made stiff against

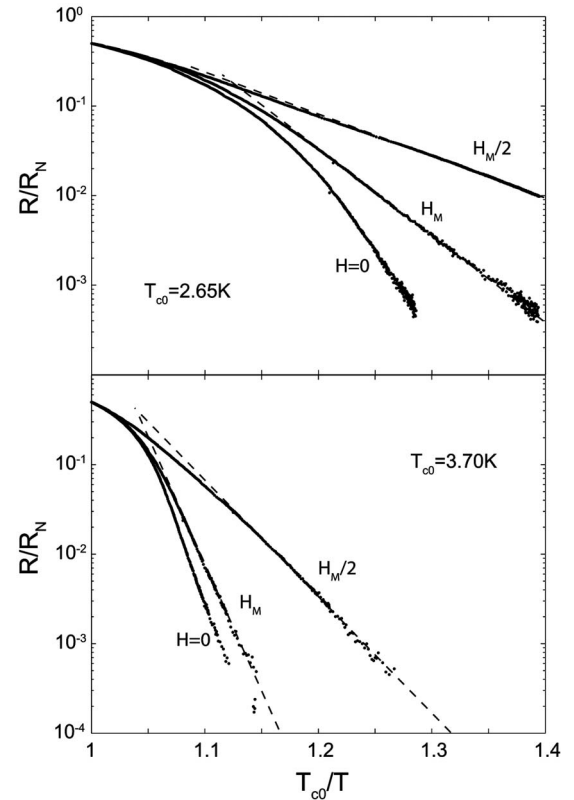


FIG. 4. Arrhenius plots for the perforated film with $R_{\text{hole}}=33$ nm. $T_{c0}=2.65$ K (top) and 3.7 K (bottom). The slope of the curve characterizes the energy barrier against vortex motion in the film. The barrier in the perforated film is nonmonotonic with field. Dashed lines are fits to Eq. (3).

thermally activated flux flow.³⁸ At half integer values of H/H_M , vortices cannot come into registry with the holes and simultaneously form a stable lattice. Consequently, the activation energy is substantially lower at incommensurate fields. That lower T_{c0} films have larger oscillation amplitudes in this regime results from the difference in the activation barriers for different T_{c0} films as seen in Fig. 4. Even on a normalized temperature scale, the lower T_{c0} film has broader transitions than the higher T_{c0} film. Correspondingly, the activation energy increases faster than linearly with T_{c0} . This behavior is consistent with the condensation energy dictating the activation energy scale. A more detailed discussion of the TAFF behavior will appear in future work.

Moving up the transition to $r > r_c$ (Fig. 3), the oscillation amplitudes wane and eventually go to zero. The behavior as $r \rightarrow r_0$ can be attributed to enhanced vortex mobility that causes them to lose registry with the holes. Nearer T_{c0} the shrinkage of the order parameter makes the barrier to inter-hole vortex motion smaller and the likelihood of amplitude fluctuations greater. Given that the constrictions in the film are quasi-one-dimensional (a few ξ_0 across) both of these effects will enhance interhole vortex motion. These effects are more pronounced in lower T_{c0} films since the condensation energy, which is proportional to T_{c0} , governs their strength. Consequently, A is lower in lower T_{c0} films.

The final regime, $r > r_0$, must connect smoothly to the normal state resistance and therefore must traverse the por-

tion of the transition where amplitude fluctuations are known to dominate.¹⁵ This necessarily implies that r_0 marks the position of two phenomena which are equivalent in a mean field description. First, it marks where the aforementioned amplitude fluctuation dominated regime ends. Second, it marks $T_c(H=H_M)$. This can be seen in the following way. To observe periodic behavior with a period corresponding to one flux quanta per unit cell, the vortices placed in each hole at the matching field must be distinct objects. As the film is cooled the vortex cores shrink as ξ approaches ξ_0 . Physically, the point at which vortices become distinct is $H_{c2}(T)$.³⁸ Above H_{c2} or $r > r_0$, “vortices” overlap and cease to exist. Therefore this regime, wherein $r > r_0$, can be characterized by amplitude fluctuations that become so strong that they destroy fluxoid quantization altogether.

Thus, even in the absence of a detailed model of $R(T)$ which accounts for fluctuations in these films, we can identify three distinct fluctuation regimes defined by r_c and r_0 . For $r < r_c$, thermally activated flux motion causes phase fluctuations. In the intermediate regime, $r_0 > r > r_c$, the vortex mobility is augmented by strong amplitude fluctuations. Finally, for $r_0 < r < 1$ amplitude fluctuations dominate and vortices do not exist.

The decrease of r_0 with T_{c0} implies that the size of the amplitude fluctuation dominated regime increases closer to

the SIT.¹¹ This trend can be attributed to the growth of both the quantum critical regime of the SIT³⁹ and the classical critical regime⁴⁰ as R_N increases. $R_N \approx R_c/2$ for the lowest T_{c0} film in the series. It suggests that the fermionic degrees of freedom strongly influence the approach to the SIT in uniform films. Experiments on lower T_{c0} , higher R_N films will provide insight into whether bosonic (vortices) or fermionic degrees of freedom dominate the SIT.

In summary, we have quench condensed nanoporated, homogeneously disordered Bi films. The regular perforations induce a phase-sensitive periodic response to an applied magnetic flux and thus provide a probe capable of distinguishing between the two types of superconducting fluctuations. In these low superfluid density films, we have found that the strength of this response crosses over between regions of the $R(T)$ dominated by fluctuations in the amplitude, $|\psi_0|$, of the superconducting order parameter to that dominated by fluctuations in the phase, ϕ . In addition, as T_{c0} is lowered and the system approaches the quantum critical point of the SIT, the region of the $R(T)$ dominated by amplitude fluctuations grows.

This work has been supported by the NSF through Grant No. DMR-0203608, AFRL, and ONR. We acknowledge helpful conversations with N. Daniilidis.

-
- ¹J. Bardeen *et al.*, Phys. Rev. **108**, 1175 (1957).
²V. J. Emery and S. A. Kivelson, Nature (London) **374**, 434 (1995).
³Z. A. Xu *et al.*, Nature (London) **406**, 486 (2000).
⁴V. Sandu *et al.*, Phys. Rev. Lett. **93**, 177005 (2004).
⁵V. N. Zavaritsky and A. S. Alexandrov, Phys. Rev. B **71**, 012502 (2005).
⁶A. F. Hebard and M. A. Paalanen, Phys. Rev. Lett. **65**, 927 (1990).
⁷A. Yazdani and A. Kapitulnik, Phys. Rev. Lett. **74**, 3037 (1995).
⁸N. Marković *et al.*, Phys. Rev. Lett. **81**, 701 (1998).
⁹L. Merchant *et al.*, Phys. Rev. B **63**, 134508 (2001).
¹⁰G. Sambandamurthy *et al.*, Phys. Rev. Lett. **92**, 107005 (2004).
¹¹J. A. Chervenak and J. M. Valles Jr., Phys. Rev. B **59**, 11209 (1999).
¹²J. M. Kosterlitz and D. J. Thouless, J. Phys. C **6**, 1181 (1973).
¹³M. R. Beasley *et al.*, Phys. Rev. Lett. **42**, 1165 (1979).
¹⁴A. F. Hebard and A. T. Fiory, Phys. Rev. Lett. **44**, 291 (1980).
¹⁵L. G. Aslamasov and A. I. Larkin, Phys. Lett. **26A**, 238 (1968).
¹⁶J. A. Chervenak and J. M. Valles Jr., Phys. Rev. B **54**, R15649 (1996).
¹⁷D. J. Resnick *et al.*, Phys. Rev. Lett. **47**, 1542 (1981).
¹⁸A. T. Fiory *et al.*, Appl. Phys. Lett. **32**, 73 (1978).
¹⁹G. S. Mkrtchyan and V. V. Shmidt, Sov. Phys. JETP **34**, 195 (1972).
²⁰U. Welp *et al.*, Phys. Rev. B **66**, 212507 (2002).
²¹A. Bezryadin and B. Pannetier, J. Low Temp. Phys. **98**, 251 (1995).
²²From SEM images we have determined the hole lattice constant $a=100\pm 5$ nm and thus $H_M=2390\pm 240$ G. The position of the peaks in the data occur at $H=2145\pm 50$ G in agreement with that calculated from the lattice constant. $H_M=2145$ G is the normalization used on the data throughout this paper.
²³M. Giroud *et al.*, J. Low Temp. Phys. **87**, 683 (1992).
²⁴H. S. J. van der Zant *et al.*, Phys. Rev. B **42**, 2647 (1990).
²⁵H. S. J. van der Zant *et al.*, Phys. Rev. B **50**, 340 (1994).
²⁶A. J. Yin *et al.*, Appl. Phys. Lett. **79**, 1039 (2001).
²⁷H. Masuda and K. Fukuda, Science **268**, 1466 (1995).
²⁸H. Masuda *et al.*, Appl. Phys. Lett. **71**, 2770 (1997).
²⁹J. Li *et al.*, Appl. Phys. Lett. **75**, 367 (1999).
³⁰X. S. Ling *et al.*, Phys. Rev. Lett. **76**, 2989 (1996).
³¹M. J. Higgins *et al.*, Phys. Rev. B **61**, R894 (2000).
³²S. Teitel and C. Jayaprakash, Phys. Rev. Lett. **51**, 1999 (1983).
³³D. Belitz and T. R. Kirkpatrick, Rev. Mod. Phys. **66**, 261 (1994).
³⁴A. M. Finkelstein, Physica B **197**, 636 (1994).
³⁵B. Pannetier *et al.*, J. Phys. (France) Lett. **44**, 853 (1983).
³⁶C. C. Abilio *et al.*, J. Low Temp. Phys. **118**, 23 (2000).
³⁷M. Hayashi and H. Ebisawa, Physica C **352**, 191 (2001).
³⁸K. Fossheim and A. Sudbo, *Superconductivity: Physics and Applications* (Wiley, West Sussex, England, 2004).
³⁹T. R. Kirkpatrick and D. Belitz, Phys. Rev. Lett. **79**, 3042 (1997).
⁴⁰N. Goldenfeld, *Lectures on Phase Transitions and the Renormalization Group* (Addison-Wesley, New York, 1992).